Oncogene (2018) 37:4679–4691
https://doi.org/10.1038/s41388-018-0283-3

ARTICLE

Molecular mechanism of the TP53-MDM2-AR-AKT signalling network regulation by USP12

Urszula L. McClurg[1,2] · Nay C. T. H. Chit[1] · Mahsa Azizyan[1] · Joanne Edwards[3] · Arash Nabbi[4] · Karl T. Riabowol[4] · Sirintra Nakjang[1,5] · Stuart R. McCracken[1] · Craig N. Robson[1]

Received: 8 May 2017 / Revised: 20 December 2017 / Accepted: 23 March 2018 / Published online: 14 May 2018

Abstract

The TP53-MDM2-AR-AKT signalling network plays a critical role in the development and progression of prostate cancer. However, the molecular mechanisms regulating this signalling network are not completely defined. By conducting transcriptome analysis, denaturing immunoprecipitations and immunopathology, we demonstrate that the TP53-MDM2-AR-AKT cross-talk is regulated by the deubiquitinating enzyme USP12 in prostate cancer. Our findings explain why USP12 is one of the 12 most commonly overexpressed cancer-associated genes located near an amplified super-enhancer. We find that USP12 deubiquitinates MDM2 and AR, which in turn controls the levels of the TP53 tumour suppressor and AR oncogene in prostate cancer. Consequently, USP12 levels are predictive not only of cancer development but also of patient's therapy resistance, relapse and survival. Therefore, our findings suggest that USP12 could serve as a promising therapeutic target in currently incurable castrate-resistant prostate cancer.

Introduction

TP53, the guardian of the genome, is a potent transcriptional regulator and a crucial tumour suppressor [1, 2]. Following ubiquitination by MDM2, TP53 is targeted for proteosomal degradation resulting in increased proliferation and tumourigenesis [3]. The ubiquitination event occurs within the nucleus. MDM2 can also directly ubiquitinate the androgen receptor (AR) leading to its degradation [4]. AR is a transcription factor critical in prostate cancer (PC) development and progression, with increased AR activity promoting prostate cell proliferation and survival. Consequently, by targeting both TP53 and AR proteins, MDM2 acts to control the balance between pro- and anti-proliferative pathways in PC.

We have previously reported that AR can be directly deubiquitinated and stabilised by ubiquitin specific peptidase 12 (USP12) [5]. USP12, when bound to its cofactors UAF1 and WDR20 [6, 7], can also deubiquitinate the AKT phosphatases PHLPP and PHLPPL [8, 9]. This activity controls the AR–AKT signalling network in which AKT can phosphorylate the AR at serines 213 and 791, which, in turn, targets it for ubiquitination by MDM2 and subsequent proteosomal degradation [4, 10]. Additionally, AKT can also phosphorylate MDM2 at serines 166 and 188, which promotes MDM2 nuclear translocation [11] and inhibits its auto-ubiquitination and proteosomal degradation [12]. Aberrant activity of AKT signalling is one of the most common features of the aggressive castrate-resistant prostate cancer (CRPC) [13–15].

Electronic supplementary material The online version of this article (https://doi.org/10.1038/s41388-018-0283-3) contains supplementary material, which is available to authorised users.

✉ Urszula L. McClurg
Urszula.McClurg@ncl.ac.uk

✉ Craig N. Robson
Craig.Robson@ncl.ac.uk

1 Newcastle Cancer Centre at the Northern Institute for Cancer Research, Newcastle University, Newcastle upon Tyne NE2 4HH, UK

2 Institute of Cell and Molecular Biosciences, Medical School, Newcastle University, Newcastle upon Tyne NE2 4HH, UK

3 Wolfson Wohl Cancer Research Centre, Institute of Cancer Sciences, College of Medical, Veterinary and Life Sciences, University of Glasgow, Glasgow G61 1QH Scotland, UK

4 Department of Oncology, Arnie Charbonneau Cancer Institute, Cumming School of Medicine, University of Calgary, Calgary T2N 4N1, Canada

5 Bioinformatics Support Unit, Faculty of Medical Sciences, Newcastle University, Newcastle upon Tyne NE2 4HH, UK

Understanding the wider network of PC regulators is now more important than ever before. PC is one of the main causes of cancer-associated deaths in males worldwide (www.wcrf.org). When localised, this disease can be managed with surgical or therapeutic intervention; however, when patients develop metastatic CRPC, there is no curative solution available [15]. Additionally, we currently lack biomarkers that would indicate which patients are more likely to develop this aggressive form of the disease. Investigating the master regulators and understanding the cellular biology of the signalling networks in PC will allow us to identify novel biomarkers and therapeutic targets in CRPC. This study demonstrates the relevance of USP12 in the development of therapy resistance and uncovers how USP12 regulates the signalling axis between critical PC master regulators, TP53-MDM2-AR-AKT, to control the balance between cellular proliferation and apoptosis. Multiple independent patient cohorts including those with end-stage PC have been assessed in this study. Our data raise the possibility that prudent combination of hormone therapy alongside inhibition of USP12 could provide a new treatment option for high-risk PC patients, who can be selectively identified and targeted for early treatment using USP12 levels as a predictive biomarker.

Results

USP12 affects multiple cellular processes

We have previously reported that USP12 plays an important role in PC cells by controlling the protein levels of the AR [5] and the AKT phosphatases, PHLPP and PHLPPL [8], to regulate the AR–AKT cross-talk. As USP12 has also been found to regulate transcription factors at the protein level, we silenced USP12 expression in LNCaP PC cells and performed RNA sequencing to further investigate its role in cellular biology. A total of 2355 genes were significantly dysregulated by USP12 silencing (Fig. 1a). Genes most affected by USP12 silencing included many cancer-related targets such as *HMGN2P46, FBN1, HES1* and *UGT2B* genes (Fig. 1b, Supplementary Figs. 1–2). Indeed, pathway analysis showed that USP12 depletion significantly affected the p53 pathway (Fig. 1c). Additionally, USP12 was found to play a role in the metabolic processes. The USP12 effect on gene expression profile was confirmed in multiple cell line models representing therapy sensitive (LNCaP), androgen independent (LNCaP-AI) and CRPC with constitutively active AR variants (CWR22Rv1). Additionally, silencing the USP12 cofactors required for its enzymatic activity, UAF-1 and WDR20 [7, 16], generally mirrored the effects of silencing USP12, confirming the role of USP12 enzymatic activity in the regulation of these transcripts (Fig. 1d–g).

USP12 regulates the expression of genes from the p53 pathway

Our pathway analysis indicated that over 40% of p53 KEGG pathway target genes were affected by USP12 depletion (Fig. 1c). KEGG pathway analysis highlighted the importance of USP12 for p53 regulated cell cycle arrest, apoptosis, DNA repair and damage prevention and p53 negative feedback signalling (Fig. 2a). Multiple p53 target genes including *BAX* were affected by USP12 silencing with 8 genes (12% of the p53 KEGG pathway) downregulated and 19 genes (28% of the p53 KEGG pathway) upregulated (Fig. 2b). Results for 89% of the genes were in agreement with the expected result of USP12 silencing on p53 levels [17]. Given the potential role of USP12 in the regulation of p53-dependent transcription, we also compared all known p53-responsive genes [18] to the list of genes identified in the USP12 regulated transcriptional network. Out of the 129 known p53-responsive genes [18], 50 (39%) were dysregulated by USP12 silencing. We have further confirmed the regulation of *BAX* by real-time qPCR in cell lines representing different stages of PC (Fig. 2c; Supplementary Fig. 3). We have also determined that additional p53 target gene *FOXO3* was significantly upregulated even though it was not identified by the initial RNA sequencing (Fig. 2c; Supplementary Fig. 3). As USP12 requires UAF1 and WDR20 complex members for its enzymatic activity, silencing any member of the USP12 complex should have comparable effects on the p53 target gene expression and this was the case in our study (Fig. 2c). While silencing USP12, or its cofactors, had no effect on *TP53* transcript levels confirming post-translational regulation by USP12 (Fig. 2c; Supplementary Fig. 3). *BAX* and *FOXO3* were significantly upregulated by USP12 silencing in LNCaP cells representing early AR positive, castration sensitive disease and also in LNCaP-AI cells representing AR positive, androgen independent disease and CWR22Rv1 cells representing late AR and AR-variant positive CRPC.

USP12 regulates p53 protein levels by deubiquitinating and stabilising MDM2 protein

Our RNA sequencing analysis indicates that upon USP12 silencing, the p53 pathway was upregulated which implies that USP12 is a negative regulator of p53. As USP12 is a deubiquitinating enzyme that has been primarily reported to deubiquitinate K48 poly-ubiquitinated proteins leading to their stabilisation, it was assumed that its effects

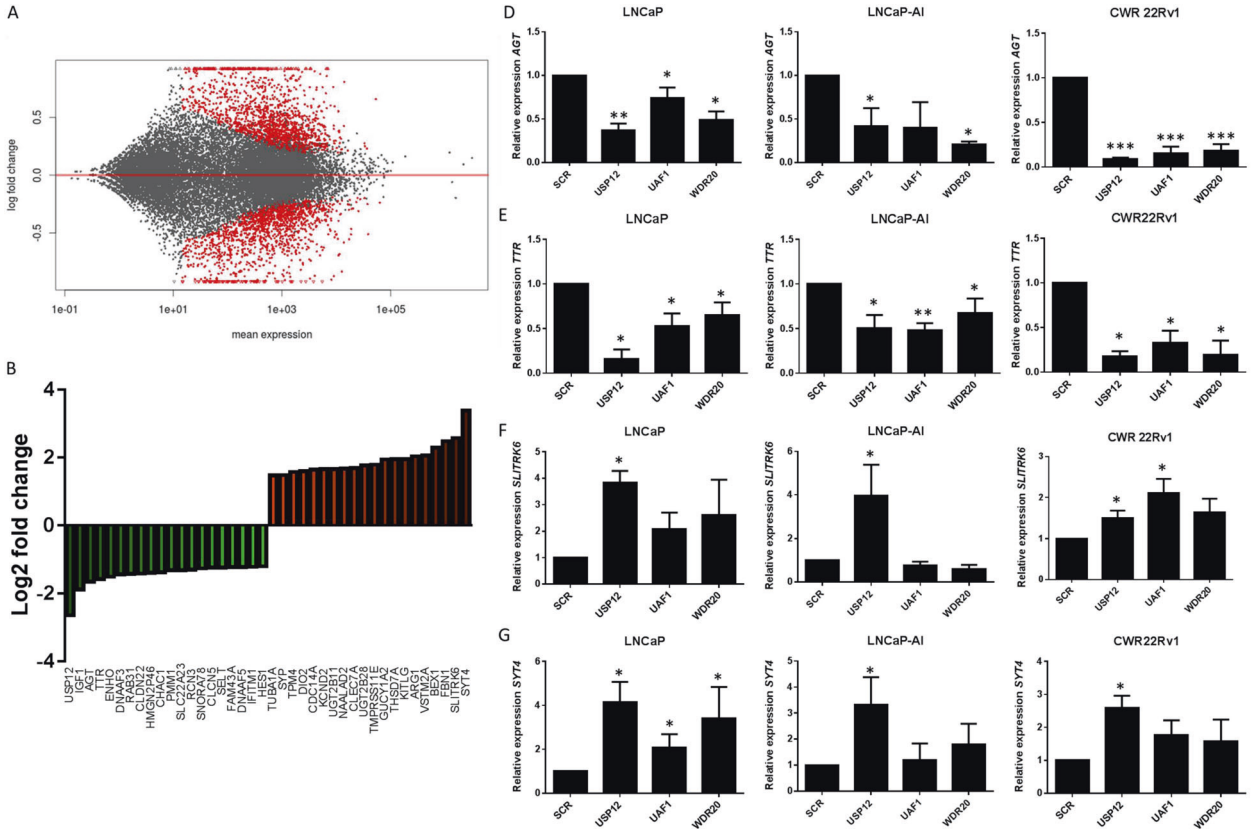

C

Pathway	over repressented p value	under repressented p value	numDEInCat	numInCat	adj p value
p53 signalling pathway	4.50E-07	0.99999	27	67	0.0001
metabolic pathways	6.09E-04	0.99956	189	1043	0.0697
Adherens junctions	1.13E-03	0.99955	23	72	0.0864
Lysosome	3.92E-03	0.99805	30	117	0.2244
Protein export	7.59E-03	0.99815	8	23	0.3476

Fig. 1 USP12 controls multiple cellular processes. **a** LNCaP cells were treated with SCR or siUSP12 siRNA for 96 h followed by RNA extraction and RNA sequencing. Transcript levels between USP12 knockdown and scrambled treated control (SCR) were compared: 2355 genes are significantly differentially expressed in siUSP12 (adjusted p value < 0.05) and marked in red. **b** Most down (green) and up (red) regulated genes following USP12 silencing. **c** Top five pathways enriched with differentially regulated genes following USP12 silencing numDEInCat: number of differentially expressed genes in the pathway; numInCat: number of genes that are part of the pathway. **d**–**g** qPCR validation of most downregulated (**d**, **e**) and upregulated (**f**, **g**) genes following 96 h USP12 silencing. LNCaP and CWR22Rv1 cells were treated with siRNA as indicated for 72 h, followed by 10 nM DHT stimulation for 24 h. LNCaP-AI cells were cultured in SDM for 96 h. Results were normalised to *HPRT1* gene expression and data are presented as mean of three independent experiments ± SEM; * indicates $p < 0.05$; ** $p < 0.01$; *** $p < 0.005$ when compared to SCR as tested with *t*-test

on p53 must be indirect. We hypothesised that USP12 exerted its effect on p53 by targeting one of the negative regulators of p53 protein for deubiquitination. Consequently, we immunoprecipitated p53's E3 ligase MDM2 from the cell lysate and discovered that USP12 was in the same cellular complex with MDM2 and p53 in cancer cells (Fig. 3a). To confirm that USP12 can interact with MDM2 in the absence of AR, we overexpressed both proteins in COS-7 cells and confirmed their interaction (Fig. 3b). Considering USP12 enzymatic activity as a deubiquitinase, we then assessed the MDM2 ubiquitination levels in PC cells following USP12 depletion. We found that USP12 silencing led to an increase in MDM2 ubiquitination, which correlated with decreased MDM2 protein levels (Fig. 3c). The proportion of ubiquitinated MDM2 increases due to the deubiquitinating enzyme USP12 being depleted, which leads to more MDM2 being degraded decreasing the total protein amount (Fig. 3c). In line with our previous data on USP12, regulation of AKT phosphatases silencing USP12 stimulated S166 phosphorylation of MDM2 (Fig. 3d). This implies that USP12 could control MDM2 by both direct deubiquitination and additionally via the AKT pathway, which regulates its autoubiquitinating ability. To further confirm that the effect of USP12 on MDM2 and consequently p53 protein levels was proteasome dependent, we silenced USP12 in the presence

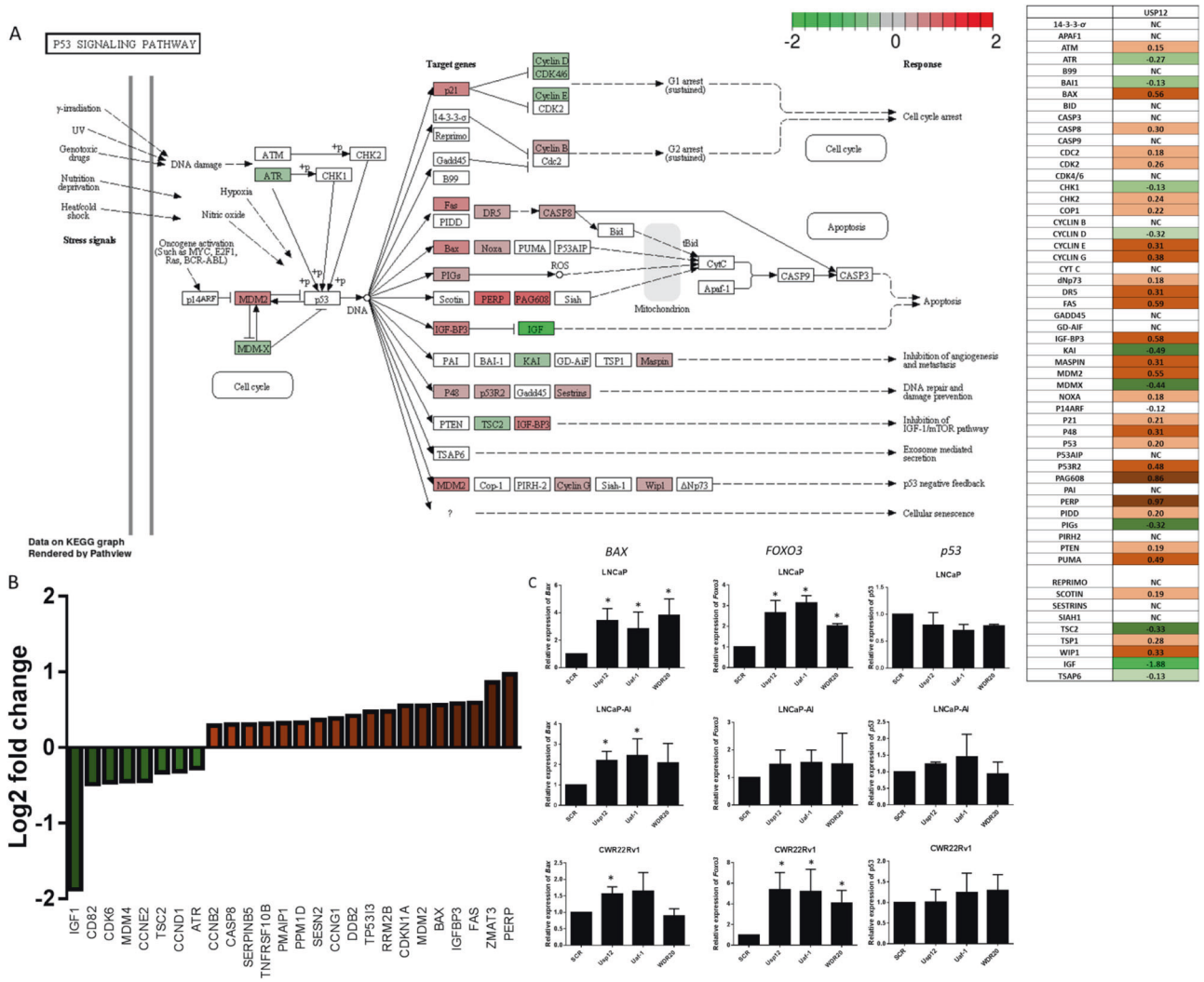

Fig. 2 USP12 controls the p53 KEGG pathway. **a** Genes from p53 KEGG pathway that were significantly altered by siUSP12 in RNA sequencing were highlighted with green to red boxes, depending on their log2FC intensities (see scale bar on the top right of the figure). **b** Histogram of differentially expressed p53 KEGG pathway genes from the RNA sequencing. **c** qPCR validation of most well-known p53 pathway genes following USP12 silencing. LNCaP and CWR22Rv1 cells were treated with siRNA as indicated for 72 h, followed by 10 nM DHT stimulation for 24 h. LNCaP-AI cells were cultured in SDM for 96 h. Results were normalised to *HPRT1* gene expression and data are presented as mean of three independent experiments ± SEM; * indicates $p < 0.05$ when compared to SCR as tested with *t*-test

and absence of the MG132 proteosome inhibitor. We observed that similar to the effect on AR, USP12 could only regulate MDM2 and p53 protein levels in the presence of an active proteasome (Fig. 3e). Finally, we confirmed the effect of USP12 silencing on p53 levels. P53 is a transcription factor which needs to translocate to the nucleus to interact with the chromatin. Upon USP12 silencing, we observed increased p53 levels in the nucleus and on the chromatin of the PC cells (Fig. 3f) explaining the increase in p53 target gene expression observed in RNA sequencing data (Fig. 2a–c). Consequently, when we immunoprecipitated p53-associated chromatin, we observed increased p53 binding to its target genes CDKN1A (Fig. 3g) and CDC20 (Fig. 3h) upon USP12 silencing.

USP12 plays a role in castration resistance

Currently, PC patients with non-curable disease are treated with anti-androgen-based therapies, after which they invariably develop a castration-resistant phenotype for which there is no available treatment beyond the minimal survival benefits seen with taxane chemotherapy [19]. Consequently, there is a need for novel drug targets in CRPC and for novel biomarkers of castration resistance. We investigated the role of USP12 in CRPC and demonstrated that USP12 silencing sensitised both castrate sensitive LNCaP cells (Fig. 4a) and androgen independent LNCaP-AI cells (Fig. 4b) to casodex, as measured by both live cell imaging and cell counts. USP12 silencing also affected the

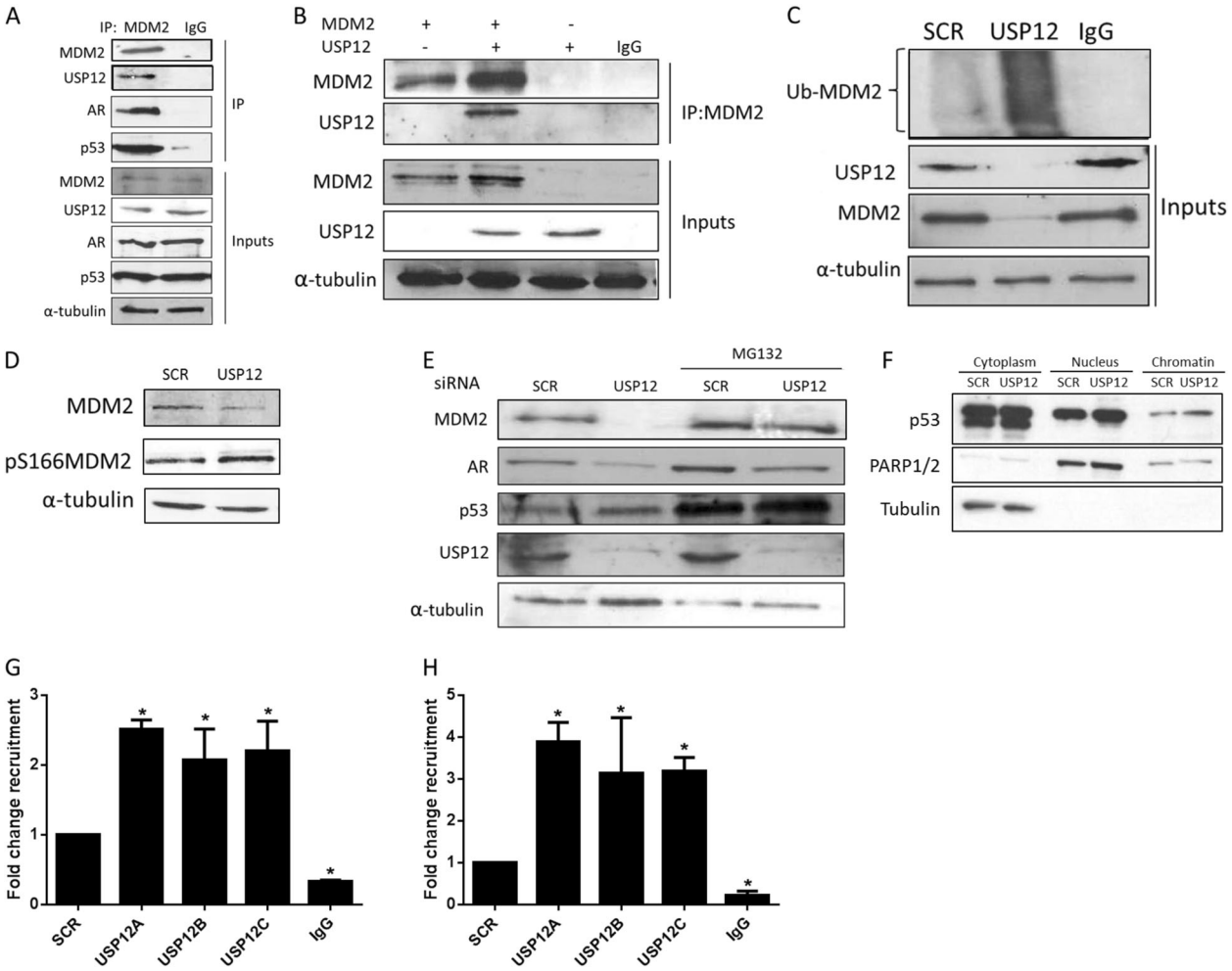

Fig. 3 USP12 controls p53 protein levels by deubiquitinating MDM2. **a** MDM2 was immunoprecipitated with interacting proteins from the LNCaP cells and immunoblotted as indicated. **b** MDM2 and USP12 were overexpressed in COS-7 cells for 72 h and MDM2 was immunoprecipitated. **c** LNCaP cells were treated with siRNA for 96 h as indicated, followed by denaturing immunoprecipitation for ubiquitinated MDM2 and immunoblotting. **d** LNCaP cells were treated with siRNA for 96 h as indicated, followed by immunoblotting. **e** LNCaP cells were treated with siRNA as indicated for 88 h followed by 8 h MG-132 treatment. **f** LNCaP cells were treated with siRNA for 96 h as indicated, followed by cellular fractionation and immunoblotting. **g**, **h** ChIP analysis of p53 recruitment to CDKN1A (**g**) and CDC20 (**h**). Data are presented as mean of three independent experiments ± SEM; * indicates $p < 0.05$ when compared to SCR as tested with ANOVA with Dunnett's multiple comparison

cellular proliferation of PC cells in the presence and absence of androgens to a degree comparable to silencing the AR itself (Fig. 4c), highlighting the potential importance of USP12 as a PC drug target in all disease stages. This effect might be due to the regulation of p53 and MDM2 by USP12 and to the regulation of AR activity, since, in the absence of USP12, the binding of AR to chromatin is significantly decreased (Fig. 4d).

USP12 is a novel biomarker of PC

As our results indicated that USP12 plays a role in PC and CRPC biology, we investigated if USP12 could be used as a biomarker of PC by assessing USP12 protein levels in clinical samples using immunohistochemistry. USP12 protein levels were significantly higher in both the cytoplasm and the nucleus of cells from patients with preneoplastic prostatic intraepithelial neoplasia (PIN). They were still higher in PC patients (Fig. 5a). This indicates that USP12 may be involved in both early and late PC development and could potentially be used to identify patients at high risk for developing PC. There was also a strong correlation (Pearson $p < 0.0001$) between the cytoplasmic and nuclear USP12 levels suggesting that USP12 might fulfil similar functions in both organelles (Fig. 5b). We further investigated the protein levels of USP12 in a large cohort of patients with benign disease compared to patients with PC. USP12 levels were significantly increased when compared to samples with benign prostatic hyperplasia (BPH) (Fig. 5c). As USP12 regulates

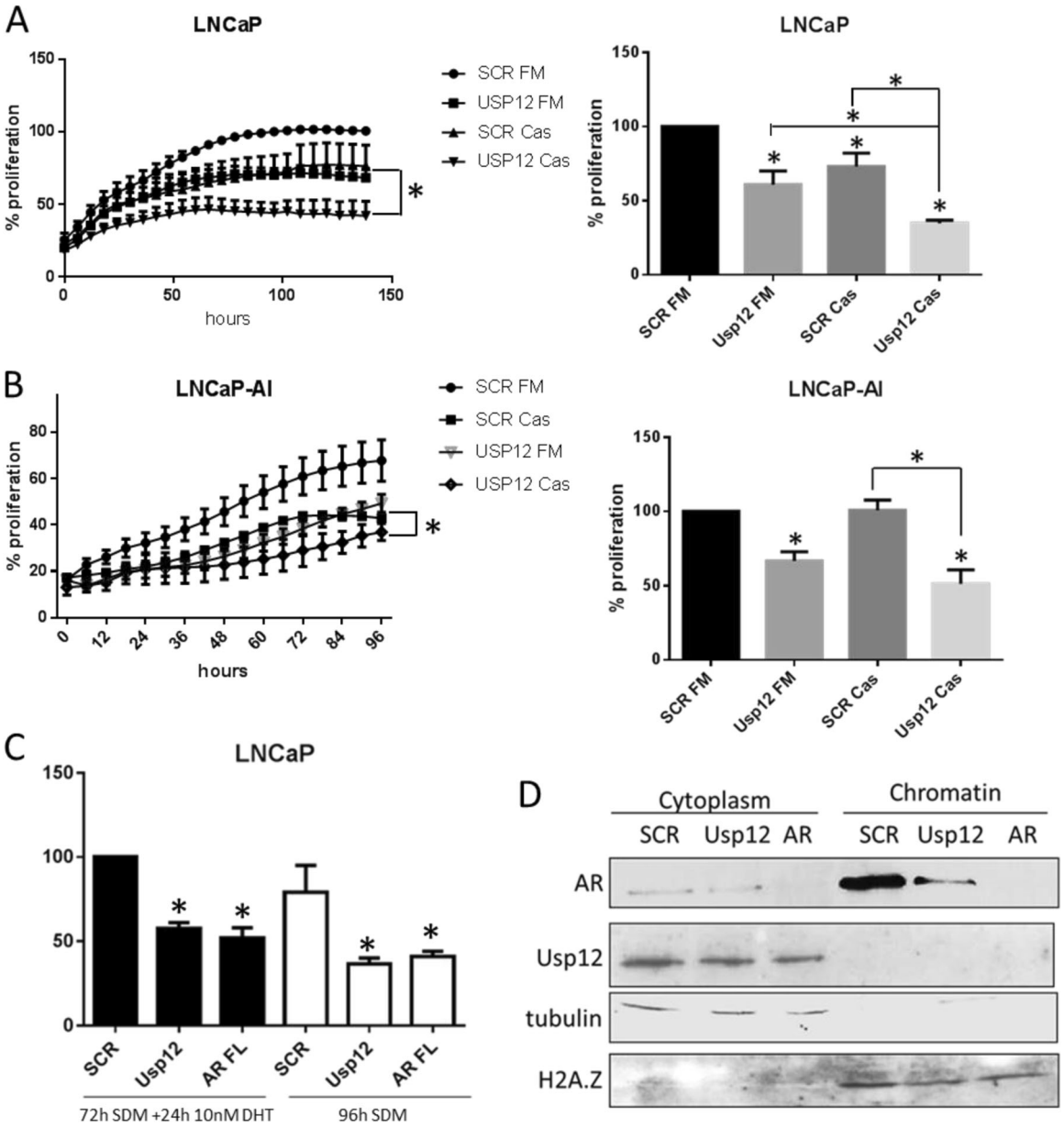

Fig. 4 USP12 controls cell growth in the presence and absence of androgens and in CRPC. LNCaP (**a**) and LNCaP-AI (**b**) cells were treated with siRNA as indicated for 96 h with and without the addition of Casodex (Cas). Cell growth was measured with live cell imaging every 6 h using the Incucyte (left side panel) and by cell counts at 96 h (right panel); * indicates $p < 0.05$ as tested with *t*-test. **c** LNCaP cells were treated with siRNA for 96 h as indicated, in the presence (black bars) and absence (white bars) of DHT followed by cell counting. Data are presented as a mean of three independent experiments ± SEM; * indicates $p < 0.05$ as tested with *t*-test. **d** LNCaP cells were treated with siRNA as indicated for 96 h, followed by cytoplasmic and chromatin extraction and immunoblotting

three most crucial pathways responsible for cell death and survival, AKT, AR and p53, we investigated USP12's correlation with the well-established proliferation marker MCM2 [20]. In our clinical cohort, the levels of USP12 and MCM2 were strongly correlated (*p* value of 0.03), supporting the idea that USP12 plays a significant role in prostate carcinogenesis (Fig. 5d). Similarly, linear regression showed a significant relationship between nuclear USP12 and MCM2 (Fig. 5e). A link between USP12 and cellular proliferation was further confirmed by a statistically significant correlation between USP12 and the Ki-67 proliferative index ($p = 0.04$; $n = 28$). We also analysed the relationship between USP12 and AR protein levels and AR target protein expression; in agreement with our cellular observations, high USP12 levels, both cytoplasmic and nuclear, correlated with increased AR (Fig. 5f, g) and prostate specific antigen (PSA) (Fig. 5h) levels in patient samples. Furthermore, confirming our cellular observations,

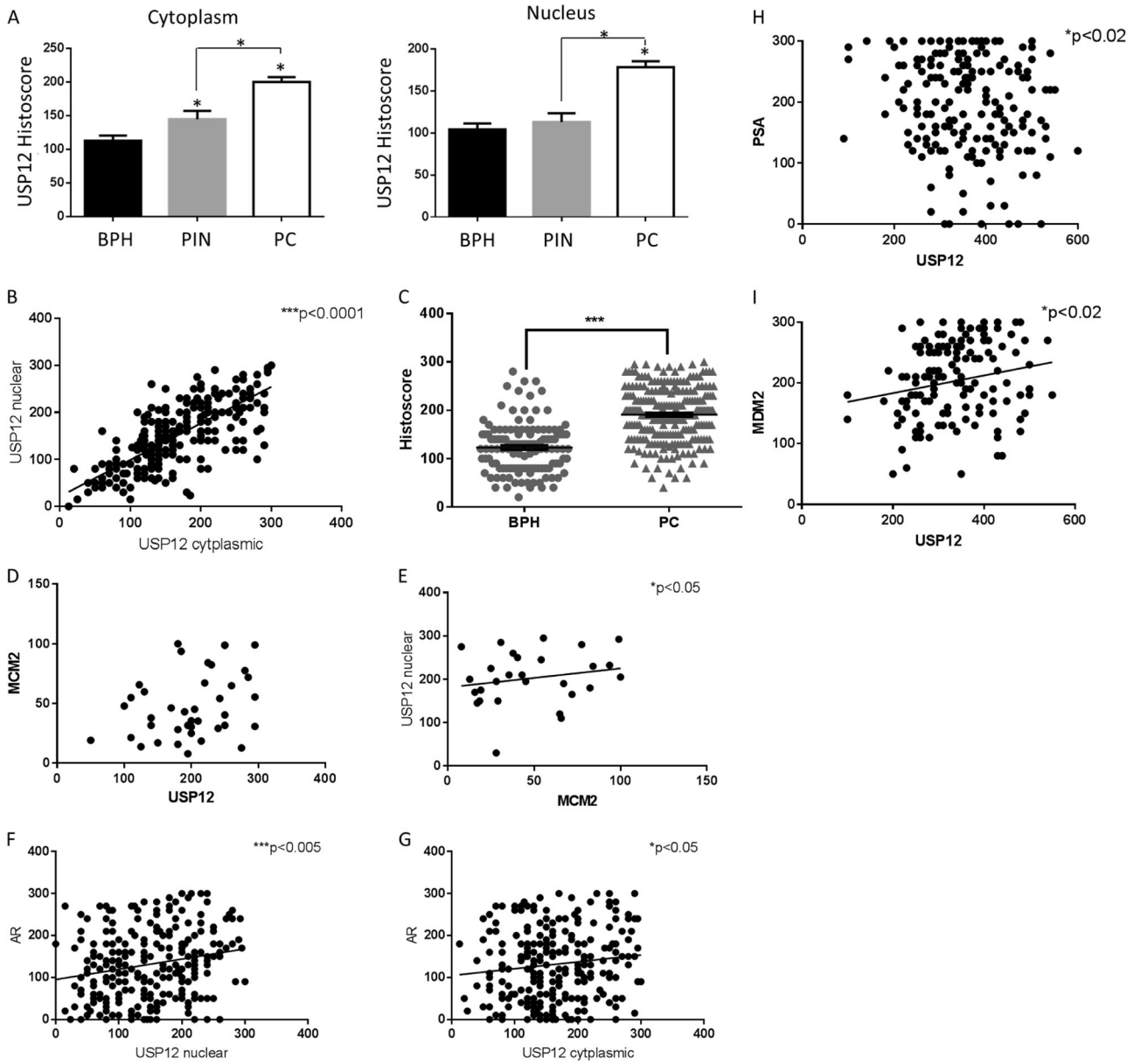

Fig. 5 USP12 is increased in PC and its levels correlate with proliferation. **a** USP12 cytoplasm and nuclear levels were assessed using histoscore in a tissue microarray (TMA) consisting of 54 benign samples (BPH), 19 pre-neoplastic samples (PIN) and 44 PC samples; * indicates $p < 0.05$ as tested with *t*-test. **b** Linear regression between cytoplasmic and nuclear USP12 levels in 254 patient cores. **c** USP12 protein levels compared between BPH ($n = 124$) and PC patient samples ($n = 251$); *** indicates $p < 0.005$ as tested with *t*-test. **d** Correlation between USP12 and MCM2 histoscores in PC samples ($n = 41$). **f**, **g** Linear regression between nuclear (**f**) and cytoplasmic (**g**) USP12 and AR levels in 254 prostate cancer tissue samples. **h** Linear regression between USP12 and PSA levels in 192 prostate cancer tissue samples. **i** Linear regression between USP12 and MDM2 levels in 138 prostate cancer tissue samples

USP12 levels were positively associated with MDM2 protein in PC (Fig. 5i).

High USP12 levels are seen in CRPC and correlate with poor prognosis in PC

Since we found that USP12 levels increase during the development of PC, we assessed USP12 as a prognostic biomarker. Patients with high USP12 levels had significantly shortened overall survival (Fig. 6a) and their time to relapse was also significantly shorter, with an average of 14.7 months in the high USP12-expressing group vs. 55.8 months in patients with low USP12 protein levels (Fig. 6b). We confirmed this by analysing the time to relapse in the TCGA cohort (http://cancergenome.nih.gov/), where high *USP12* transcript levels were also predictive of shorter

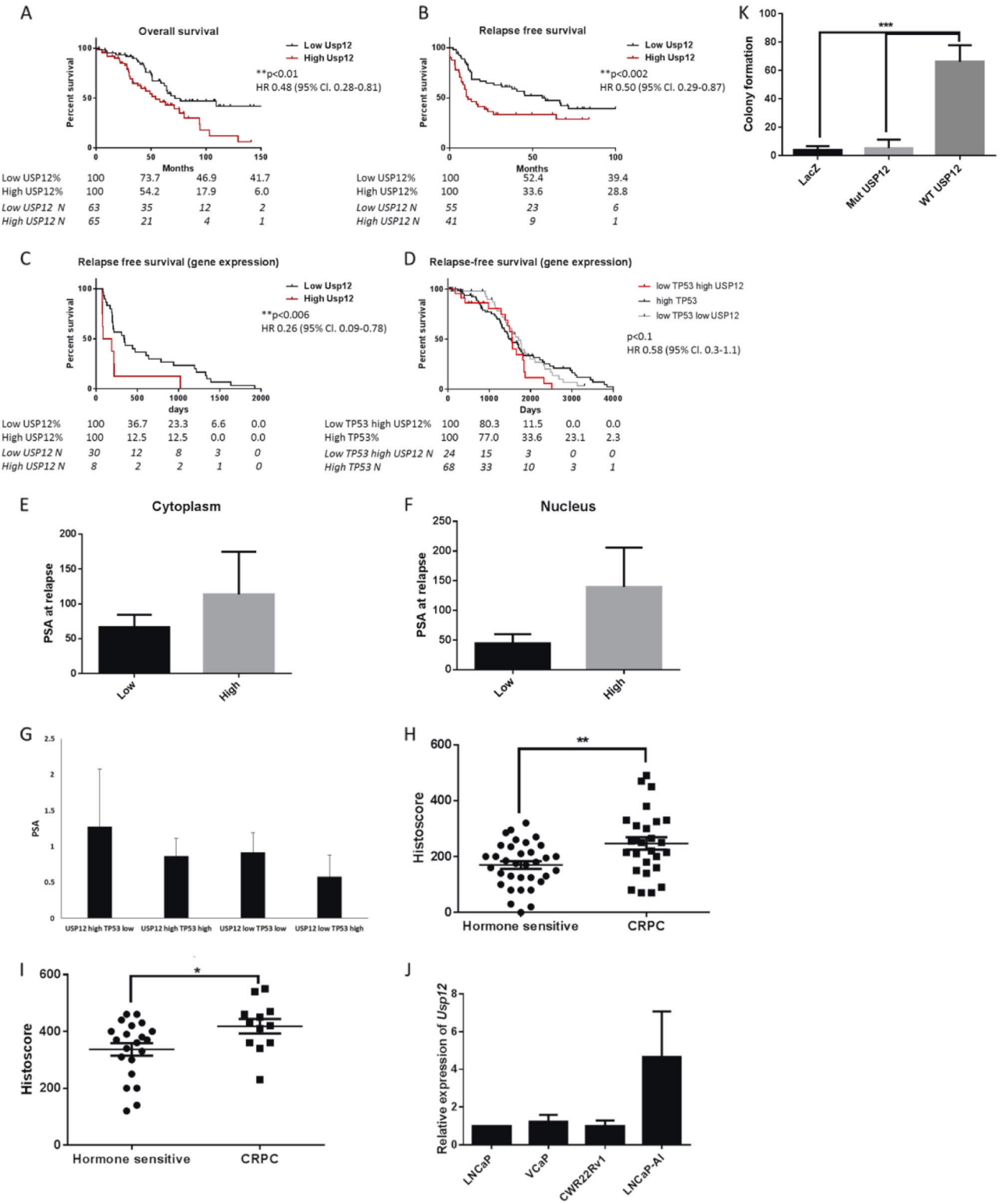

relapse-free survival (Fig. 6c). Similarly, when we divided the patients based on their *USP12* and *TP53* expression, the patients with low *TP53* and high *USP12* had the most aggressive disease while patients with high *TP53* experienced the longest relapse-free survival, this difference was not significant due to our small sample number but it showed a trend. Low *TP53*- and low *USP12*-expressing patients had medium survival (Fig. 6d). Furthermore,

◀ **Fig. 6** USP12 is a marker of poor prognosis in PC. **a** PC patient overall survival based on USP12 protein levels ($n = 128$). **b** PC relapse-free survival based on USP12 protein levels ($n = 99$). **c** PC relapse-free survival based on *USP12* gene expression (TCGA) ($n = 38$). **d** PC relapse-free survival based on *USP12* and *TP53* gene expression (TCGA) ($n = 142$). Italicised number of subjects still at risk (*N*) indicates the patients still remaining in the study and is deducted by both patients who died/relapsed and patients who were censored after withdrawing from the study. **e**, **f** Patients PSA at relapse based on USP12 cytoplasm ($n = 13$) (**e**) and nuclear ($n = 13$) (**f**) levels. **g** PSA levels of TCGA patient cohort were divided based on their *USP12* and *TP53* levels. **h**, **i** USP12 histoscore comparison between hormone-sensitive and CRPC patients in Newcastle ($n = 33$) (**h**) and Glasgow ($n = 61$) (**i**) cohort. The samples were independently assessed for nuclear and cytoplasmic staining on a 0–300 scale and combined cellular histoscore of 0–600 was created; * indicates $p < 0.05$; ** $p < 0.01$ as tested with *t*-test. **j** Comparison of *USP12* transcript levels between cell lines representing different stages of PC. **k** LNCaP cells lentivirally transduced with either LacZ control, C48A enzymatically dead USP12 or WT USP12 were cultured in SDM media for 14 days, followed by crystal violet staining and colony formation count. Data are presented as mean of three independent experiments ± SEM; *** indicates $p < 0.005$ as tested with ANOVA with Dunnett's multiple comparison

patients with high USP12, both cytoplasmic (Fig. 6e) and nuclear (Fig. 6f), had higher PSA levels at relapse. Additionally, when we analysed the TCGA patient cohort PSA results based on their *USP12* and *TP53* levels, we observed highest PSA in the group with high *USP12* and low *TP53* and lowest PSA in the group with low *USP12* and high *TP53* confirming the link between TP53 regulation by USP12 and PC (Fig. 6g). Furthermore, when we compared the USP12 levels between hormone-sensitive and CRPC patients from our North of England, UK cohort, we found that they were significantly increased with disease progression (Fig. 6h). Similarly, in patients from an independent cohort [21], CRPC patients had increased USP12 protein compared to treatment sensitive disease (Fig. 6i). This was further confirmed in our cell line models. For example, our real-time qPCR analysis indicated that androgen independent LNCaP-AI cells had significantly increased *USP12* transcript levels compared to their parental androgen sensitive line, indicating that USP12 might be involved in the CRPC biology in this model (Fig. 6j). As we previously reported that silencing USP12 significantly decreases the ability of LNCaP-AI cells to grow in steroid deplete conditions [5, 8], we investigated if overexpression of USP12 could drive androgen independence. To answer this, we analysed colony formation in the absence of androgens in LNCaP cells overexpressing WT USP12 or enzymatically dead USP12 mutant. Cells overexpressing WT USP12 had significantly increased ability to form colonies in the absence of steroids, compared to control or mutant USP12 overexpressing cells (Fig. 6k).

Discussion

Progression to castrate-resistant disease is a major challenge of translational PC research. Currently, the median time to progression is approximately 18 months and survival typically does not extend beyond 12 months after the development of metastatic CRPC [15], [22]. Even the recent development of second and third line anti-androgens has only reinforced our understanding that resistance development is unavoidable and multifactorial with second and third line treatment only offering short-term survival advantage [23, 24]. Hence, it is crucial for us to understand the mechanisms through which resistance develops and to identify the signalling networks that control AR activity and CRPC development. Our study outlines USP12 as a novel master regulator of the critical signalling axis TP53-MDM2-AR-AKT, which plays a role in PC development and subsequently progression to CRPC.

Deubiquitinating enzymes have been at the forefront of research in recent years, with critical roles in cancer biology becoming evident [25]. Here we report that USP12 plays a role as a master regulator in PC by controlling the TP53-MDM2-AR-AKT signalling network that is responsible for prostate tumour development and progression (Supplementary Fig. 5). USP12 controls AKT by targeting PHLPPs [8], the most commonly mutated genes in early PC [26]. USP12 also deubiquitinates both AR and MDM2, which in turn controls TP53 levels. We also demonstrate that USP12 is required for cell growth and AR activity at all stages of the disease, even in the castrate environment. This is a promising discovery as DUBs have recently been successfully explored as therapeutic targets. USP1, which similarly to USP12, depends on a WD40 protein binding for its enzymatic activity [27], was found to play a role in cisplatin resistance [28, 29]. Inhibitors targeting the interaction between USP1 and its cofactor have been developed which have enabled high specificity. This approach has been very successful in treating cisplatin-resistant lung cancer and is currently in clinical trials [30–33]. Similar observations have been made in osteosarcoma where USP1 was observed to be overexpressed and its subsequent depletion decreased proliferation and invasion [34]. In glioblastoma, USP1 overexpression was found to promote therapy resistance [35]. Targeting USP12 might be particularly beneficial in neuroendocrine PCs where a recent tri-centre study (Trento, Cornell and Broad) accessible through TCGA (http://cancergenome.nih.gov/) reported that 17% of the analysed tumours had USP12 amplification (13 of 77 samples) [36]. USP12 targeting might also prove useful in other epithelial cancers as it has recently been identified to be one of the 12 most commonly overexpressed cancer-associated genes located near an amplified super-enhancer [37]. In this study, we report that besides targeting the AR, USP12

deubiquitinates both MDM2 and PHLPPs controlling the protein levels of p53 and pAKT, highlighting its potential utility in anti-cancer therapy design. Recent developments in targeting the USP1-UAF1 interaction for USP1 inhibition highlighted the importance of understanding the DUB-WD40 complex structure in specific therapeutics design [38]. Recently the USP12-UAF1 structure has been solved, allowing for similar approaches to be undertaken [39, 40].

We used multiple models to evaluate our observations using cell lines that represent distinct disease stages, including androgen-sensitive PC, androgen-independent PC with full length AR and CPRC with full length AR and constitutively active AR variants. We also validated our results using patient samples from our in-house cohort containing end-stage disease, an independent patient cohort and publically available large datasets. All of our sample sets confirmed that USP12 plays a critical role in early PC development and in the onset of incurable castrate-resistant disease. This, taken together with recent advances in DUB targeting therapeutics and the frequency of USP12 amplifications in PC, highlights the potential of USP12 as a novel therapeutic target.

Materials and methods

Antibodies and plasmids

Anti-AR (Santa Cruz Biotechnology; N20 clone), anti-H2A.Z [41], anti-MDM2 (Santa Cruz N20 and SMP14), anti-FLAG, anti-USP12 and anti-α-tubulin (Sigma), anti-p53 (Dako) and anti-ubiquitin (Santa Cruz Biotechnology) were included in this project. Plasmids used were pMYC-MDM2, pFLAG-USP12 [5].

Cell culture, transfections

LNCaP, CWR22Rv1 and COS-7 cells (all purchased from the ATCC) and LNCaP-AI variant cell line derived in-house [42] were cultured in RPMI 1640 medium with 2 mM L-glutamine (Invitrogen) supplemented with 10% (v/v) foetal calf serum (FCS) or steroid depleted serum (SDM) at 37 °C in 5% CO_2. Cell lines were never maintained for more than 30 passages or 2 months of continuous culturing. As per institutional policy, cell lines were authenticated and tested for mycoplasma on a tri-monthly basis. Transfections were performed using TransIT-LT1 reagent (MirusBio) following the manufacturer's instructions. The ViraPower Lentiviral Expression system (Life Sciences) was used to generate viral particles using pLenti-USP12 or enzymatically dead mutant C48A USP12 [5] expression vectors and control pLenti-LacZ vector (Life Sciences).

Immunoprecipitation (IP)

Cells were seeded at 10^6 cells/90-mm dish, transfected with 1 µg of plasmid when indicated, incubated for 48 h, and lysed directly into lysis buffer (50 mM Tris, pH 7.5, 150 mM NaCl, 0.2 mM Na_3VO_4, 1% Nonidet P-40, 1 mM PMSF, 1 mM DTT, and 1× protease inhibitors (Roche Applied Science)). Lysates were incubated with 1 µg of antibodies for 16 h at 4 °C, and antibodies were pulled down using protein G-Sepharose beads (Invitrogen). For denaturing IPs, cells were subjected to 20 µM MG132 proteasomal inhibitor treatment for the final 8 h, followed by collection into lysis buffer supplemented with 2% SDS and subsequently denatured at 100 °C for 10 min [5] prior to immunoprecipitation.

For chromatin isolation, cells were trypsinised and resuspended in 1 ml of buffer A (10 mM HEPES pH 7.9, 10 mM KCl, 1.5 mM $MgCl_2$, 0.34 M sucrose, 10% glycerol, 1 mM DTT and 1× protease inhibitors cocktail) on ice for 10 min. Nuclei were collected by centrifugation at 1200×*g* for 5 min at 4 °C. The cytosolic fraction was cleared by centrifugation at 200×*g* for 5 min at 4 °C. Nuclei were washed in 1 ml of buffer A without glycerol and resuspended in 1 ml of buffer B (3 mM EDTA, 0.2 mM EGTA, 1 mM DTT and 1× protease inhibitor cocktail) on ice for 30 min. Finally, the sample was centrifuged at 1500×*g* for 5 min at 4 °C and the chromatin pellet was washed in buffer B seven times [43].

siRNA gene silencing and gene expression analysis

Cells were reverse transfected with siRNA using RNAiMax (Invitrogen) according to the manufacturer's instructions and incubated in culture medium for 96 h prior to cell lysis. siRNA sequences were as follows SCR: UUCUCCGAACGUGUCACGU[dT][dT]; AR: CCAUCUUUCUGAAUGUCCU[dTdT]; USP12: CAGAUCUCUUCCAUAGCAU[dTdT], WDR20: CGAGAAAGAUCACAAGCGA[dTdT] and UAF1: CAAAUUGGUUCUCAGUAGA[dTdT] [7]. Routinely, we achieved >60%, >65% and >80% knockdown for UAF1, WDR20 and USP12, respectively, in qPCR validation [7] (Supplementary Fig. 1). We also used additional USP12 targeting sequences USP12 A GAAACUCUGUGCAGUGAAU[dTdT] and USP12 C AUCAGAUAUCUCAAAGAA[dTdT] described previously [5]. For RNA sequencing, RNA was extracted using the QIAGEN RNeasy Plus Mini Kit, and all the samples from three separate biological experiments were sequenced using Illumina's total stranded RNA prep kit with ribozero gold for library preparation with 100 bp paired end reads on the Illumina HiSeq 2500 platform, performed by AROS.

Reads were mapped to the reference human genome hg19 using STAR2-pass allowing up to two mismatches [44]. Per gene raw read counts for each sample were obtained using HTseq and Gencode version 19 [45]. Gene-level differential expression analysis was performed using DEseq2 [46]. *p*-Values were adjusted to control for the false discovery rate (FDR) using the Benjamini–Hochberg method. Differentially expressed genes from each comparison were tested for functionally enriched pathways and gene ontology terms using GOseq [47] with a gene length bias correction on pathways annotated in KEGG database. Gene expression fold changes within KEGG pathways were visualised using the R package pathview [48].

Proliferation analysis

For proliferation analysis, IncuCyte measurements of cellular occupation of the wells were taken every 6 h, and additionally in a separate set of experiments, the cell numbers were counted at 96 h to assess cellular proliferation [8].

Immunohistochemistry

Tissue microarrays (TMA) containing 0.6 mm cores of BPH, PIN, PC and control tissues including breast, kidney, placenta, ovary and liver were used from retrospective cohorts. Antigens were retrieved by pressure cooking in 10 mM citrate pH 6.0 (Supplementary Fig. 4). The TMAs were independently scored by two individuals using the 0–300 H-score method [49]. Briefly, percentage and intensity of staining for positive cells was estimated (0, 1, 2, 3) using the following equation: H-score = (% of cells with low level positivity) + 2×(% of cells with medium level positivity) + 3×(% of cells with high level positivity). All sections were scored blinded. For survival analysis, high marker levels were defined as a value in the third and fourth upper quarter of the population [50, 51].

qPCR

For qPCR RNA was extracted using Trizol (Invitrogen) according to manufacturer's instruction, and quantified using Nanodrop. cDNA synthesis using the oligo dT primers and data analysis was performed as described previously [8]. Briefly, 1 µg of RNA was reverse transcribed with 1 U of MMLV reverse transcriptase, 50 ng Oligo-dT and 630 µM dNTP (Promega). qPCR was performed using the relative quantification method on three independent biological experiments and each sample was loaded in triplicate. qRT-PCR was conducted using SYBR®Green on 384-well optical reaction plates with the ABI 7900HT real-time PCR system. Results were normalised to *HPRT1* expression. Primers were *HPRT1* F: 5′-GAACGTCTTGCTCGAGAGATGTG-3′, R: 5′-CCAG-CAGGTCAGCAAAGAATTT-3′; *BAX* F: GCCCTT TTGCTTCAGGGTTTCA, R: TCAGCTTCTTGGTG-GACGCA; *FOXO3 F:* AACGTGGGGAACTTCACTGGT, R: TTTGAGGGTCTGCTTTGCCCA; *AGT* F: CCCCAGT CTGAGATGGCTC, R: GACGAGGTGGAAGGGGTG TA; *TTR* F: TGGGAGCCATTTGCCTCTG, R: AGCCG TGGTGGAATAGGAGTA; *SYT4* F: ATGGGATACCCT ACACCCAAAT, R: TCCCGAGAGAGGAATTAGAAC TT; *SLTRK6* F: TCCAGTGCTCTCATCCAGAGG, R: AGTTGGAAAGGTCGTGATGGT.

Colony formation

LNCaP cells carrying pLenti-LacZ, pLenti-WT USP12 or pLenti- C48A USP12. Cells were seeded in SDM at 2000 cells per well in a 6-well plate and allowed to form colonies. After 14 days, the cells were stained with crystal violet and the colonies were counted [7].

Chromatin immunoprecipitation (ChIP)

ChIPs were performed as described previously [7]. LNCaP cells were transfected with siRNA for 96 h. Data are presented as percentage input using the following formula: % input = 100 × AE (amplification efficiency)×(CT adjusted input sample − CT immunoprecipitated sample). CT refers to cycle threshold. CDKN1 A F: CTGTGGCTCTGAT TGGCTTTCT; R: GACAAAATAGCCACCAGCCTCT, CDC20 F: CCGCTAGACTCTCGTGATAGC; R: TGGC TCCTTCAAAATCCAAC.

Statistics

Data were tested for normal distribution and variance similarity, and appropriate statistics were applied as detailed in the figure legends.

Acknowledgements ULM, SRM and CNR were funded by PC UK (PG09-23), JGWP Foundation (BH142412) and JRE Scientific Committee Charity, Newcastle Healthcare Charity (JG/ML/0414). CNR is supported by Cancer Research UK (C27826/A15994). NCTHC was funded by Newcastle University.

Author contributions ULM and CNR designed the study; ULM, NCTHC and MA performed the experiments; ULM and SRM scored and analysed all of the pathology data, ULM, AN and KTR analysed the TCGA dataset; SN and ULM analysed the RNA sequencing data; JE provided the Glasgow patient cohort; ULM prepared the manuscript with input from all authors.

Compliance with ethical standards

Conflict of interest The authors declare that they have no conflict of interest.

References

1. Brown CJ, Lain S, Verma CS, Fersht AR, Lane DP. Awakening guardian angels: drugging the p53 pathway. Nat Rev Cancer. 2009;9:862–73.
2. Poletto M, Legrand AJ, Fletcher SC, Dianov GL. p53 coordinates base excision repair to prevent genomic instability. Nucleic Acids Res. 2016;44:3165–75.
3. Fuchs SY, Adler V, Buschmann T, Wu X, Ronai Z. Mdm2 association with p53 targets its ubiquitination. Oncogene. 1998;17:2543–7.
4. Lin HK, Wang L, Hu YC, Altuwaijri S, Chang C. Phosphorylation-dependent ubiquitylation and degradation of androgen receptor by Akt require Mdm2 E3 ligase. EMBO J. 2002;21:4037–48.
5. Burska UL, Harle VJ, Coffey K, Darby S, Ramsey H, O'Neill D, et al. Deubiquitinating enzyme USP12 is a novel co-activator of the Androgen Receptor. J Biol Chem. 2013;288:32641–50.
6. Sowa ME, Bennett EJ, Gygi SP, Harper JW. Defining the human deubiquitinating enzyme interaction landscape. Cell. 2009;138:389–403.
7. McClurg UL, Harle VJ, Nabbi A, Batalha-Pereira A, Walker S, Coffey K, et al. Ubiquitin-specific protease 12 interacting partners UAF-1 and WDR20 are potential therapeutic targets in prostate cancer. Oncotarget. 2015;6:37724–26.
8. McClurg UL, Summerscales EE, Harle VJ, Gaughan L, Robson CN. Deubiquitinating enzyme USP12 regulates the interaction between the androgen receptor and the AKT pathway. Oncotarget. 2014;5:7081–92.
9. Brognard J, Sierecki E, Gao T, Newton AC. PHLPP and a second isoform, PHLPP2, differentially attenuate the amplitude of Akt signaling by regulating distinct Akt isoforms. Mol Cell. 2007;25:917–31.
10. Lin HK, Yeh S, Kang HY, Chang C. Akt suppresses androgen-induced apoptosis by phosphorylating and inhibiting androgen receptor. Proc Natl Acad Sci USA. 2001;98:7200–5.
11. Mayo LD, Donner DB. A phosphatidylinositol 3-kinase/Akt pathway promotes translocation of Mdm2 from the cytoplasm to the nucleus. Proc Natl Acad Sci USA. 2001;98:11598–603.
12. Feng J, Tamaskovic R, Yang Z, Brazil DP, Merlo A, Hess D, et al. Stabilization of Mdm2 via decreased ubiquitination is mediated by protein kinase B/Akt-dependent phosphorylation. J Biol Chem. 2004;279:35510–7.
13. Edwards J, Krishna NS, Witton CJ, Bartlett JM. Gene amplifications associated with the development of hormone-resistant prostate cancer. Clin Cancer Res. 2003;9:5271–81.
14. Marques RB, Aghai A, de Ridder CM, Stuurman D, Hoeben S, Boer A, et al. High efficacy of combination therapy using PI3K/AKT inhibitors with androgen deprivation in prostate cancer preclinical models. Eur Urol. 2014;67:1177–85.
15. Feldman BJ, Feldman D. The development of androgen-independent prostate cancer. Nat Rev Cancer. 2001;1:34–45.
16. Kee Y, Yang K, Cohn MA, Haas W, Gygi SP, D'Andrea AD. WDR20 regulates activity of the USP12 x UAF1 deubiquitinating enzyme complex. J Biol Chem. 2010;285:11252–7.
17. Mirza A, Wu Q, Wang L, McClanahan T, Bishop WR, Gheyas F, et al. Global transcriptional program of p53 target genes during the process of apoptosis and cell cycle progression. Oncogene. 2003;22:3645–54.
18. Riley T, Sontag E, Chen P, Levine A. Transcriptional control of human p53-regulated genes. Nat Rev Mol Cell Biol. 2008;9:402–12.
19. Tannock IF, de Wit R, Berry WR, Horti J, Pluzanska A, Chi KN, et al. Docetaxel plus prednisone or mitoxantrone plus prednisone for advanced prostate cancer. New Engl J Med. 2004;351:1502–12.
20. Joshi S, Watkins J, Gazinska P, Brown JP, Gillett CE, Grigoriadis A, et al. Digital imaging in the immunohistochemical evaluation of the proliferation markers Ki67, MCM2 and Geminin, in early breast cancer, and their putative prognostic value. BMC Cancer. 2015;15:546.
21. Willder JM, Heng SJ, McCall P, Adams CE, Tannahill C, Fyffe G, et al. Androgen receptor phosphorylation at serine 515 by Cdk1 predicts biochemical relapse in prostate cancer patients. Br J Cancer. 2013;108:139–48.
22. Lohiya V, Aragon-Ching JB, Sonpavde G. Role of chemotherapy and mechanisms of resistance to chemotherapy in metastatic castration-resistant prostate cancer. Clin Med Insights Oncol. 2016;10:57–66. Suppl 1
23. Attard G, Antonarakis ES. Prostate cancer: AR aberrations and resistance to abiraterone or enzalutamide. Nat Rev Urol. 2016;13:697–8.
24. Antonarakis ES, Lu C, Wang H, Luber B, Nakazawa M, Roeser JC, et al. AR-V7 and resistance to enzalutamide and abiraterone in prostate cancer. N Engl J Med. 2014;371:1028–38.
25. McClurg UL, Robson CN. Deubiquitinating enzymes as oncotargets. Oncotarget. 2015;6:9657–68.
26. Xiong X, Li X, Wen YA, Gao T. Pleckstrin Homology (PH) domain leucine-rich repeat protein phosphatase controls cell polarity by negatively regulating the activity of atypical protein kinase C. J Biol Chem. 2016;291:25167–78.
27. Murai J, Yang K, Dejsuphong D, Hirota K, Takeda S, D'Andrea AD. The USP1/UAF1 complex promotes double-strand break repair through homologous recombination. Mol Cell Biol. 2011;31:2462–9.
28. Sourisseau T, Helissey C, Lefebvre C, Ponsonnailles F, Malka-Mahieu H, Olaussen KA, et al. Translational regulation of the mRNA encoding the ubiquitin peptidase USP1 involved in the DNA damage response as a determinant of Cisplatin resistance. Cell Cycle. 2016;15:295–302.
29. Zhiqiang Z, Qinghui Y, Yongqiang Z, Jian Z, Xin Z, Haiying M, et al. USP1 regulates AKT phosphorylation by modulating the stability of PHLPP1 in lung cancer cells. J Cancer Res Clin Oncol. 2012;138:1231–8.
30. Chen J, Dexheimer TS, Ai Y, Liang Q, Villamil MA, Inglese J, et al. Selective and cell-active inhibitors of the USP1/ UAF1 deubiquitinase complex reverse cisplatin resistance in non-small cell lung cancer cells. Chem Biol. 2011;18:1390–400.
31. Dexheimer TS, Rosenthal AS, Liang Q, Chen J, Villamil MA, Kerns EH, et al.Discovery of ML323 as a Novel Inhibitor of the USP1/UAF1 Deubiquitinase Complex. Probe Reports from the NIH Molecular Libraries Program. Bethesda, MD: NIH Molecular Libraries Programme; 2010.
32. Dexheimer TS, Rosenthal AS, Luci DK, Liang Q, Villamil MA, Chen J, et al. Synthesis and structure-activity relationship studies of N-benzyl-2-phenylpyrimidin-4-amine derivatives as potent USP1/UAF1 deubiquitinase inhibitors with anticancer activity against nonsmall cell lung cancer. J Med Chem. 2014;57:8099–110.
33. Mistry H, Hsieh G, Buhrlage SJ, Huang M, Park E, Cuny GD, et al. Small-molecule inhibitors of USP1 target ID1 degradation in leukemic cells. Mol Cancer Ther. 2013;12:2651–62.
34. Liu J, Zhu H, Zhong N, Jiang Z, Xu L, Deng Y, et al. Gene silencing of USP1 by lentivirus effectively inhibits proliferation and invasion of human osteosarcoma cells. Int J Oncol. 2016;49:2549–57.
35. Lee JK, Chang N, Yoon Y, Yang H, Cho H, Kim E, et al. USP1 targeting impedes GBM growth by inhibiting stem cell maintenance and radioresistance. Neuro Oncol. 2016;18:37–47.

36. Beltran H, Prandi D, Mosquera JM, Benelli M, Puca L, Cyrta J, et al. Divergent clonal evolution of castration-resistant neuroendocrine prostate cancer. Nat Med. 2016;22:298–305.
37. Zhang X, Choi PS, Francis JM, Imielinski M, Watanabe H, Cherniack AD, et al. Identification of focally amplified lineage-specific super-enhancers in human epithelial cancers. Nat Genet. 2016;48:176–82.
38. Wahi D, Jamal S, Goyal S, Singh A, Jain R, Rana P, et al. Cheminformatics models based on machine learning approaches for design of USP1/UAF1 abrogators as anticancer agents. Syst Synth Biol. 2015;9:33–43.
39. Dharadhar S, Clerici M, van Dijk WJ, Fish A, Sixma TK. A conserved two-step binding for the UAF1 regulator to the USP12 deubiquitinating enzyme. J Struct Biol. 2016;196:437–47.
40. Li H, Lim KS, Kim H, Hinds TR, Jo U, Mao H, et al. Allosteric activation of ubiquitin-specific proteases by beta-propeller proteins UAF1 and WDR20. Mol Cell. 2016;63:249–60.
41. Binda O, Sevilla A, LeRoy G, Lemischka IR, Garcia BA, Richard S. SETD6 monomethylates H2AZ on lysine 7 and is required for the maintenance of embryonic stem cell self-renewal. Epigenetics. 2013;8:177–83.
42. Rigas AC, Robson CN, Curtin NJ. Therapeutic potential of CDK inhibitor NU2058 in androgen-independent prostate cancer. Oncogene. 2007;26:7611–9.
43. McClurg UL, Cork DM, Darby S, Ryan-Munden CA, Nakjang S, Mendes Cortes L, et al. Identification of a novel K311 ubiquitination site critical for androgen receptor transcriptional activity. Nucleic Acids Res. 2017;45:1793–804.
44. Dobin A, Davis CA, Schlesinger F, Drenkow J, Zaleski C, Jha S, et al. STAR: ultrafast universal RNA-seq aligner. Bioinformatics. 2013;29:15–21.
45. Anders S, Pyl PT, Huber W. HTSeq--a Python framework to work with high-throughput sequencing data. Bioinformatics. 2015;31:166–9.
46. Love MI, Huber W, Anders S. Moderated estimation of fold change and dispersion for RNA-seq data with DESeq2. Genome Biol. 2014;15:550.
47. Young MD, Wakefield MJ, Smyth GK, Oshlack A. Gene ontology analysis for RNA-seq: accounting for selection bias. Genome Biol. 2010;11:R14.
48. Luo W, Brouwer C. Pathview: an R/Bioconductor package for pathway-based data integration and visualization. Bioinformatics. 2013;29:1830–1.
49. Kirkegaard T, Edwards J, Tovey S, McGlynn LM, Krishna SN, Mukherjee R, et al. Observer variation in immunohistochemical analysis of protein expression, time for a change? Histopathology. 2006;48:787–94.
50. Pei H, Li L, Fridley BL, Jenkins GD, Kalari KR, Lingle W, et al. FKBP51 affects cancer cell response to chemotherapy by negatively regulating Akt. Cancer Cell. 2009;16:259–66.
51. Chen M, Pratt CP, Zeeman ME, Schultz N, Taylor BS, O'Neill A, Castillo-Martin M, et al. Identification of PHLPP1 as a tumor suppressor reveals the role of feedback activation in PTEN-mutant prostate cancer progression. Cancer Cell. 2011;20:173–86.